Carbohydrate Polymers 96 (2013) 528–535

Contents lists available at SciVerse ScienceDirect

Carbohydrate Polymers

journal homepage: www.elsevier.com/locate/carbpol

Polysaccharide-based polyelectrolytes hollow microcapsules constructed by layer-by-layer technique

Yifeng Zhang[a,b], Cong Chen[a], Jianguo Wang[a,c], Lina Zhang[a,*]

[a] Department of Chemistry, Wuhan University, Wuhan 430072, China
[b] Glyn O. Phillips Hydrocolloid Research Center at HUT, Hubei University of Technology, Wuhan 430068, China
[c] College of Food Science and Engineering, Northwest A&F University, Yangling, Shaanxi 712100, China

ARTICLE INFO

Article history:
Received 17 November 2012
Received in revised form 30 March 2013
Accepted 10 April 2013
Available online 18 April 2013

Keywords:
Carboxymethylated polysaccharide
Quaternized polysaccharide
ZnO microspheres
Layer-by-layer assembly
Hollow microcapsules

ABSTRACT

Two water-soluble polysaccharide derivatives, carboxymethylated and quarternized glucans (CMGP and QGP) were synthesized for the first time from water-insoluble polysaccharides (GP) extracted from *Ganoderma lucidum*. Hollow microspheres were constructed using electrostatic layer-by-layer (LbL) deposition of the CMGP and QGP polyelectrolytes onto colloidal ZnO particles followed by the core decomposition with an acid solution. The structures of the multilayered CMGP/QGP microspheres were investigated by transmission electron microscopy (TEM), zeta potential and dynamic light scattering (DLS). The results revealed that the multilayer thickness increased regularly from 48 to 145 nm as the number of deposited CMGP/QGP layers was increased from two to seven, and the mean increment of thickness was ~25 nm per layer, reflecting the high regularity of the layer-by-layer assembly. This work provided an easy method to construct hollow microcapsules with biocompatibility and controlled dimensions.

1. Introduction

Layer-by-layer assembly by alternating adsorption is a powerful approach for the construction of multilayered films on solid substrates (Decher, 1997). Compared with the other techniques of creating ultra-thin membranes, LbL has many advantages such as the broad selection of membrane material, including synthetic polyelectrolytes (Ackern, Krasemann, & Tieke, 1998; Decher, Hong, & Schmitt, 1992; Ferreira, Cheung, & Rubner, 1994; He et al., 1999; Laschewsky et al., 1996), charged organic molecules (Ariga, Lvov, & Kunitake, 1997; Lvov, Kamau, Zhou, & Rusling, 1999; Van Cott et al., 2002; Zhang, Gao, Kong, Sun, & Shen, 1994), organic/inorganic particles (Ostrander, Mamedov, & Kotov, 2001; Rogach, Koktysh, Harrison, & Kotov, 2000; Schmitt et al., 1997; Sun et al., 1997; Wang, Sasaki, et al., 2003; Wang, Xing, Xu, & Yu, 2003) as well as charged biomacromolecules (Caruso, Caruso, & Möhwald, 1998a; Caruso, Furlong, Ariga, Ichinose, & Kunitake, 1998b; Caruso, Lichtenfeld, Giersig, & Möhwald, 1998c; Jiang & Liu, 2004; Kong et al., 1994; Lvov, Lu, Schenkman, Zu, & Rusling, 1998; Serizawa, Yamaguchi, & Akashi, 2003; Taton, Mucic, Mirkin, & Letsinger, 2000; Thierry, Winnik, Merhi, Silver, & Tabrizian, 2003; Zhou & Li, 2004). The multilayered ultra-thin films can be assembled from biomacromolecules in aqueous solution at room temperature, leading to the retention of the native chain conformation. In addition, in this approach there is no need to consider the influence of the substrate structure on the film-forming biomacromolecules, which can ensure the bioactivity to the maximum extent. Therefore, LbL technology has been extensively used in the biomedical field (Chluba et al., 2001; Chung & Rubner, 2002; Lvov & Sukhorukov, 1997; Lvov et al., 1998; Pei, Cui, Yang, & Wang, 2001; Qiu, Leporatti, Donath, & Möhwald, 2001; Vázquez, Dewitt, Hammond, & Lynn, 2002).

Hollow microcapsules fabricated via the LbL self-assembly of oppositely charged polyelectrolytes have a good prospect in a wide range of applications. Donath et al. have pioneered the research on the construction of hollow capsules by colloid-templated consecutive polyelectrolyte adsorptions followed by the decomposition of the templating core (Donath, Sukhorukov, Caruso, Davis, & Möhwald, 1998). The use of removable, charged colloidal particles as assembly templates for the sequential deposition of polyelectrolytes allowed the fabrication of three-dimensional hollow polymer shells. By applying the electrostatic self-assembly strategy, a variety of polyelectrolyte systems with novel structures have been investigated (Caruso, Caruso, et al., 1998; Caruso, Furlong, et al., 1998; Caruso, Lichtenfeld, et al., 1998; Donath et al., 1998; Sukhorukov, Donath, Davis, et al., 1998; Sukhorukov, Donath, Lichtenfeld, et al., 1998; Sun & Chu, 2009; Zhu, Zhang, Wu, & Shen, 2002), leading to great practical applications. Generally, synthetic polymers are the most commonly used as the wall material in electrostatic LbL assembly, such as poly (allylamine

* Corresponding author. Tel.: +86 27 87219274; fax: +86 27 68762005.
E-mail addresses: lnzhang@public.wh.hb.cn, linazhangwhu@gmail.com (L. Zhang).

0144-8617/$ – see front matter © 2013 Elsevier Ltd. All rights reserved.
http://dx.doi.org/10.1016/j.carbpol.2013.04.016

hydrochloride) (PAH), sodium polystyrene sulfonate (PSS) and poly (diallyldimethylammonium chloride) (PDADMAC). However, these synthetic polymers have serious disadvantages for potential biomedical applications due to their non-biocompatibility and non-biodegradability (Hiller, Leporatti, Schnäckel, Typlt, & Donath, 2004). Thus, multilayered materials constructed from biopolymers have attracted considerable attention in recent years. Ladet and his colleagues have reported the fabrication of the multilayered onion-like hydrogels of chitosan by changing the balance between hydrophilic and hydrophobic interactions (Ladet, David, & Domard, 2008). This novel multilayered, complex architecture with highly controlled physical properties holds great promise in both the fields of tissue engineering and drug delivery (Elisseeff, 2008). In our laboratory, ampholytic hydrogels with pH and salt responsive properties have been synthesized by cross-linking quaternized cellulose and carboxymethyl cellulose. When the number of fixed positive charges is equal to that of fixed negative charges in the hydrogel, strong electrostatic attractions occur in the hydrogel networks, resulting in a dense network structure (Chang, He, Zhou, & Zhang, 2011). Therefore, the oppositely charged polysaccharide-based polyelectrolytes could be assembled into multilayered structure by electrostatic attraction. The construction of the microcapsules prepared from natural polymers is an important objective. These microcapsules from natural polymers have not only excellent release properties but also good biocompatibility and biodegradability.

In our previous work, a linear water-insoluble β-(1 → 3)-D-glucan has been obtained from the fruiting bodies of *Ganoderma lucidum* (Wang & Zhang, 2009). It has been reported that *G. lucidum* polysaccharides and their derivatives have significant immunomodulatory effects and anti-tumor activity (Cao & Lin, 2002; Wang, Zhang, Yu, & Cheung, 2009), as a result of the ability of specific binding to a variety of cell surface receptors in human (Czop & Austen, 1985a; Czop & Austen, 1985b; Czop & Kay, 1991). We are interested in chemical modification of this linear polysaccharide by carboxymethylation and quaternization, respectively, to prepare the oppositely charged derivatives with water-solubility, and to construct microcapsules through electrostatic layer-by-layer self-assembly in water. On the basis of the excellent characteristics of non-toxic side effects (Li, Li, Wu, Ong, & Loutfy, 2009) and easy removal with dilute acetic acid, we selected ZnO microspheres as the colloidal template to construct core–shell composite microspheres. The hollow capsules can be obtained by dissolving the ZnO cores. The hollow microcapsules prepared from the polysaccharides-based polyelectrolytes should have excellent biocompatibility and safety, which makes it a good candidate for potential applications in the biomedical fields.

2. Experimental

2.1. Chemicals and materials

3-Chloro-2-hydroxypropyltrimethylammonium chloride (CHPTAC) and chloroacetic acid were purchased from Guofeng Fine Chemical Co., Ltd., and Sinopharm Chemical Reagent Co., Ltd., respectively. Zinc acetate dihydrate ($Zn(Ac)_2{\cdot}2H_2O$), diethylene glycol and other analytical-grade chemical reagents were purchased in China, and used as received without further purification. Ultrapure water used in all experiments and for all cleaning steps was obtained by a Milli-Q water purification system (Millipore) and had a resistivity higher than 18.2 MΩ cm.

A linear water-insoluble β-(1 → 3)-D-glucan was extracted from the fruit body of *G. lucidum* (gift from Longyan College in Fujian, China) according to our previous method (Wang & Zhang, 2009). The defatted fruit body powder was immersed stepwise in 0.9% aqueous NaCl at 25 °C, 40 °C and 95 °C, respectively. The mixture was mechanical stirred for 24 h in each step. The resultant residue was extracted with 1 M NaOH aqueous for 8 h at 40 °C, the extraction was centrifugated and then the supernatant was neutralized by acetic acid. The precipitation was collected and washed with distilled water ten times, then lyophilized to get a white powder. The polysaccharide was dissolved in dimethylsulfoxide (DMSO) at 25 °C overnight with stirring and then centrifuged to remove the insoluble substance. The supernatant was dialyzed by using regenerated cellulose tubes (M_w cut-off 8000, USA) against tap water for five days and distilled water for three days to obtain the white precipitate, which was the pure sample. The pure sample was lyophilized with a lyophilizer (Christ Alpha 1-2, Osterode am Harz, Germany) to give the white powder, coded as GP, which was the same as GL-IV-I in reference (Wang & Zhang, 2009).

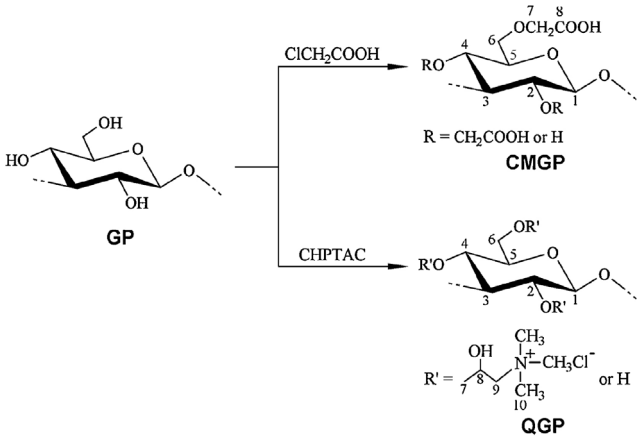

Fig. 1. Reaction scheme of carboxymethylation (CMGP) and quaternization (QGP) of *Ganoderma lucidum* (GP) in NaOH aqueous solution.

2.2. Preparation of polysaccharide derivatives

The derivatization reaction strategy is shown schematically in Fig. 1. From the water-insoluble GP sample, water-soluble carboxymethylated polysaccharide was firstly synthesized. 500 mg of the polysaccharide GP was suspended in 15 mL of isopropanol at room temperature. To the mixture, 10 mL of 30% aqueous NaOH solution was slowly added within 10 min with vigorous stirring for 90 min, then 3 g of chloroacetic acid was added. Subsequently, the mixture was allowed to react for 2 h at 50 °C. The reacted mixture was delaminated and then neutralized with HCl to give a homogeneous solution of the carboxymethylated polysaccharide. The resultant derivative solution was dialyzed against tap water for five days and then distilled water for three days. Finally, the solution was lyophilized to get the white scale-like carboxymethylated glucan sample, coded as CMGP, which was a polyelectrolyte.

Into a 100 mL round bottom flask, 2 g of GP was dissolved in 20 mL of 1 M NaOH aqueous solution at room temperature, and then 4 mL of aqueous CHPTAC solution was added dropwise into the polysaccharide solution. The mixture was reacted at 70 °C for 3 h under N_2 protection. The reacted product was neutralized with aqueous HCl, and dialyzed against distilled water for seven days to give the quarternized polysaccharide solution. The solution was finally lyophilized to obtain the quaternized polysaccharide derivative, coded as QGP, which was a polyelectrolyte.

2.3. Preparation of ZnO microspheres

For the synthesis of the ZnO microspheres, 120 mL of diethylene glycol and 3 g of zinc acetate dihydrate were added into a 250 mL

round bottom flask. The mixture was heated to 150 °C under magnetic stirring until zinc acetate dihydrate completely dissolved. The solution was heated to 180 °C and reacted for 2 h. Subsequently, the milky-white reacted product was cooled in an ice bath and then centrifuged. The precipitate was washed with absolute alcohol, 50% (v/v) ethanol/water solution and water, respectively, and finally lyophilized to obtain white ZnO microspheres.

2.4. Stepwise deposition of polysaccharide-based polyelectrolyte

Typical alternating adsorption conditions were used to create the polyelectrolyte multilayers on the colloidal ZnO microspheres, i.e., 1 mg/mL of the polyelectrolyte (CMGP or QGP) in 0.5 M NaCl, and ZnO particle concentration of 1.5 wt%. The adsorption time was 20 min. Centrifugation speeds of 6000 rpm were more than sufficient to settle the polyelectrolyte-coated particles. Prior to the addition of the next polyelectrolyte, the particles were washed three times with ultrapure water to ensure complete removal of the non-adsorbed polyelectrolytes.

In order to achieve stepwise deposition of the CMGP/QGP polyelectrolytes on the colloidal particles, positively charged ZnO microspheres were initially suspended in negatively charged CMGP aqueous solution. After electrostatic adsorption, the excess CMGP molecules were removed by three-time centrifugation and washing with ultrapure water. The next layer deposition was carried out with positively charged QGP aqueous solution via the same procedure. Consecutively, alternating adsorption of oppositely charged polyelectrolyte layers was carried on until the desired number of layers was deposited.

2.5. Fabrication of hollow microcapsules

After four bilayers of CMGP/QGP had been deposited onto the colloidal ZnO particle, the composite microspheres ZnO/$(CMGP/QGP)_4$ were treated with 0.1 M acetic acid solution. With the HAc solution added dropwise, the core was decomposed immediately, as evidenced by the fact that the initially milk-white suspension became essentially transparent within a few seconds. The mixture solution was then dialyzed against tap water for five days and ultrapure water for three days to remove the excess acid and the ZnO degradation products, and finally lyophilized to obtain the hollow microcapsules, which consist only of polysaccharide-based polyelectrolytes.

2.6. Characterizations

Fourier-Transform Infrared Spectra (FTIR) of the native polysaccharide and its derivatives were recorded on a Nicolet 170SX FTIR (Spectrum One, Perkin Elmer Co., USA) spectrometer in the range of 4000–400 cm^{-1} using the KBr-disk method. ^{13}C NMR measurements of the samples were analyzed on a Mercury 600 NMR spectrometer (Varian Inc., USA) at room temperature. The concentrations of GP and its derivatives were adjusted to 80 mg/mL for NMR experiments. DMSO-d_6 was used as the solvent for GP and 99.96% D_2O was used as the solvent for the derivatives, respectively.

Transmission electron microscopy (TEM) of the colloidal ZnO microspheres was carried out with a JEOL JEM-2010 (HT) electron microscope at an accelerating voltage of 200 kV. High-resolution transmission electron microscopy (HRTEM) image was taken on a JEOL JEM 2010 FEF (UHR) microscope at 200 kV. Scanning electron microscopy (SEM) measurements were performed with a FESEM (SEM, SIRION TMP, FEI) operated at an accelerating voltage of 20 kV. The surface of the specimens for SEM observations was sputter-coated with about 5 nm of Au film under vacuum, and then observed and photographed.

The zeta potentials of ZnO microspheres alternately coated with CMGP and QGP were measured using Zetasizer Nano-ZS (Malvern Instruments, UK) in ultrapure water at 25 °C. All measurements were performed in triplicate. Mean values and corresponding standard deviations (mean ± SD) were shown as results.

The viscosity of the polysaccharide derivatives in water was determined by using an Ubbelodhe capillary viscometer at 25 °C. The kinetic energy correction was always negligible. The Huggins equation was used to estimate the intrinsic viscosity ($[\eta]$) value by extrapolation of concentration (c) to zero as follows (Huggins, 1942),

$$\frac{\eta_{sp}}{c} = [\eta] + k[\eta]^2 c \quad (1)$$

where η_{sp}/c is the reduced specific viscosity, and k is the constant for a given polymer in given conditions.

A modified commercial instrument consisted of an ALV/DLS/SLS-5000E light scattering goniometer (ALV/CGS-8F, ALV, Germany) with vertically polarized incident light of wavelength 632.8 nm from a He–Ne laser equipped with an ALV/LSE-5003 light scattering electronics and multiple tau digital correlator was used to measure the hydrodynamic radius (R_h) and the hydrodynamic radius distribution $f(R_h)$ for the colloidal ZnO particles and the microspheres alternately deposited with eight-layer polyelectrolytes [ZnO/$(CMGP/QGP)_4$] in water at 25 °C. The normalized autocorrelation function $g^{(2)}(t,q)$ of scattered light intensity, which related to the z-average translational diffusion coefficient D_z and $q(4\pi n \sin(\theta/2)/\lambda_0)$ was measured at 90°. The R_h value was calculated with the Stokes–Einstein relation as follows (Zhang et al., 2000),

$$R_h = \frac{k_B T}{6\pi\eta_0 Dz} \quad (2)$$

where k_B, T and η_0 denote the Boltzmann's constant, absolute temperature and the solvent viscosity, respectively. The hydrodynamic radius distribution $f(R_h)$ can also be calculated from the Laplace inversion of the measured intensity–intensity time correlation function $G^{(2)}(t)$ by using the CONTIN program.

3. Results and discussion

3.1. Chemical structure of CMGP and QGP

G. lucidum polysaccharide (GP) was water-insoluble, whereas its derivatives, CMGP and QGP, were water-soluble. Fig. 2a shows the IR spectra of GP and its derivatives. All samples displayed a significant absorption at 3400 cm^{-1}, which is due to the stretching vibration of -OH. There was a significant absorption at 890 cm^{-1}, which is the key characteristic peak of the β-glycosidic bond, indicating that the GP and its derivatives were from β-D-glucan (Kiho, Sakushima, Wang, Nagai, & Ukai, 1991). For CMGP, there were two new absorption peaks at 1620 and 1430 cm^{-1}, which were attributed to the asymmetric stretching vibration of -COOH and the symmetric stretching vibration of -COOH, respectively (Wang, Zhang, & Ruan, 2004; Zhang, Zhang, Chen, & Zeng, 2001). In the IR spectra of QGP, new characteristic absorption peaks appeared at 1480 cm^{-1} and 1417 cm^{-1}, which were assigned, respectively, to characteristic absorption peak of the methyl ($-CH_3$) in quaternary ammonium groups (Loubaki, Ourevitch, & Sicsic, 1991) and the stretching vibration peak of C–N in quaternary ammonium groups (Kacurakova, Ebringerova, Hirsch, & Hromadkova, 1994; Pal, Mal, & Singh, 2005). The results of IR indicated that the derivatization of GP were completed to give carboxymethylated and quaternized glucans. To further characterize their structure, ^{13}C NMR measurements were carried out. Fig. 2b shows the ^{13}C NMR spectra of GP and its derivatives of CMGP and QGP. The original polysaccharide

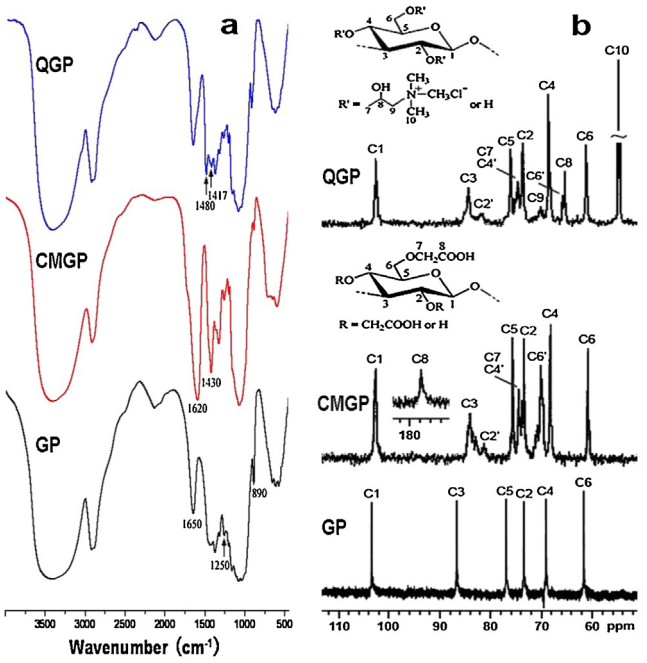

Fig. 2. (a) FT-IR spectra of native GP and its derivatives CMGP and QGP. (b) ^{13}C NMR spectra of GP in DMSO-d_6, CMGP and QGP in D_2O.

GP contained only six uniform peaks, at 103.7, 86.8, 77.0, 73.5, 69.1 and 61.5 ppm, which were attributed to C1, C3, C5, C2, C4 and C6 of β-D-glucan, respectively. This result was consistent with the literature, indicating that the GP was a linear β-(1 → 3)-D-glucan (Colson, Jennings, & Smith, 1974). Usually, the linear β-(1 → 3)-D-glucan is water-insoluble, because the side chains contribute mainly to the solvation of polysaccharide in aqueous solution, whereas the backbone is relatively hydrophobic. Compared with the GP, the ^{13}C NMR spectrum of the anionic polysaccharide CMGP exhibited a clear signal peak at δ = 177.8 ppm, attributed to the C=O carbon. Meanwhile, the signals at δ = 70.0 ppm, 74.4 ppm and 81.3 ppm were attributed to substituted C6′, C4′ and C2′, respectively. Fig. 2b also shows the ^{13}C NMR spectrum of the cationic polysaccharide QGP. The chemical shift of 102.6 ppm corresponding to C1 was shifted to lower field due to the influence of derivatization. The peaks at 84.1, 75.7, 73.4, 68.2 and 60.8 ppm were attributed to C3, C5, C2, C4 and C6, respectively. The peaks of C2′, C4′ and C6′ substituted by quaternary ammonium were at 81.7, 74.3 and 65.5 ppm, respectively. The peaks of C7, C8 and C9 were at 74.3, 65.0 and 69.7 ppm, respectively. The strongest peak at 54.3 ppm was attributed to the methyl carbon of $(CH_3)_3N^+$. The NMR results further confirmed that QGP was the quaternary ammonium cationic derivatives of GP, and CMGP was carboxymethylated glucan. In view of these results, it can be concluded that the water-soluble anionic and cationic polysaccharides (CMGP and QGP) were synthesized successfully from the water insoluble polysaccharides of *G. lucidum*.

3.2. Electrostatic force between CMGP and QGP

It is well known that the intrinsic viscosity is a measure of the hydrodynamic volume of macromolecules, and it can reflect the extent of the expansion of the polymer chains by electrostatic repulsion (Mitchell, 1979; Lapasin & Pricl, 1995). In plots of reduced viscosity versus polyelectrolyte concentration, there is usually a change in slope in the extremely dilute concentration regime (Fuoss & Strauss, 1948). As shown in Fig. 3, the reduced viscosity (η_{sp}/c) of the two kinds of derivatives (CMGP and QGP) increased significantly with a decrease in the concentration (c),

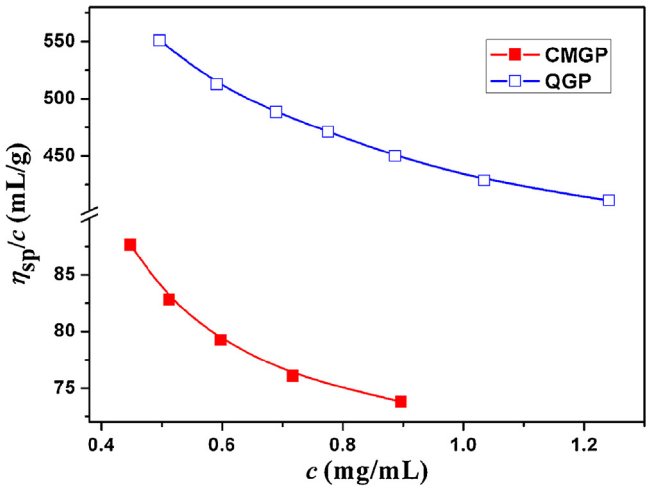

Fig. 3. Plots of reduced viscosity (η_{sp}/c) against concentration (c) of polysaccharide-based polyelectrolytes in pure water at 25 °C.

indicating the typical electrostatic repulsion effects of the polyelectrolytes in water. The introduction of the carboxyl methyl or quaternary ammonium groups through derivatization, resulted in the polyelectrolytes with negative charge or with positive charge. There was the mutual repulsion between the groups with similar charge in the polyelectrolyte chains in pure water. The electrostatic repulsion between the similarly charged groups led to the expansion of the polyelectrolyte chains. Thus the η_{sp}/c value rapidly increased upon the dilution of the polymer solution (Zhou et al., 2001). From the results in Fig. 3, the η_{sp}/c values of QGP were much more than that of CMGP, indicating that the QGP chains exhibited relatively large electrostatic force and stiffness.

3.3. Structure and size of the ZnO colloidal particles

Zinc acetate was used as the precursor. The product generated by solvothermal reaction at 180 °C was centrifuged to discard the supernatant, subsequently anhydrous ethanol was added and then ultrasonic dispersed into suspension for thorough cleaning. This step was repeated twice, after which the white ZnO powder was obtained by freeze-drying. Fig. 4a and b shows the TEM images of the sample thus prepared. Clearly, there existed a wide distribution of the ZnO microspheres diameters ranging from 400 to 1100 nm. Fig. 4d shows the typical energy-dispersive spectrum (EDS) of the ZnO microspheres, indicating the presence of only elements Zn and O (the element Cu arose from the copper grid), and further confirming that the product was ZnO. The selected area electron diffraction (SAED) in Fig. 4c shows the typical diffraction circles, corresponding to (100), (002), (101), (102), (003) and (110) planes (Wang, Sasaki, et al., 2003; Wang, Xing, et al., 2003). This indicated that the microspheres were wurtzite ZnO.

Fig. 4e shows the SEM results of the ZnO particles. The particles exhibited a better spherical morphology. Our statistical analysis revealed that the average microsphere size was 712 ± 119 nm, consistent with that in the TEM. It indicated that we have successfully fabricated ZnO microspheres by the solvothermal method.

3.4. Construction of ZnO/CMGP/QGP microspheres

The LbL self-assembly technique was used to consecutively deposit the oppositely charged CMGP and QGP on the surface of the ZnO particles, rendering the formation of core–shell composite ZnO/(CMGP/QGP)$_4$ microspheres with the ZnO particles as the core and the multilayer polyelectrolytes of CMGP and QGP as the shell. The main driving force in the alternate adsorption was thought to

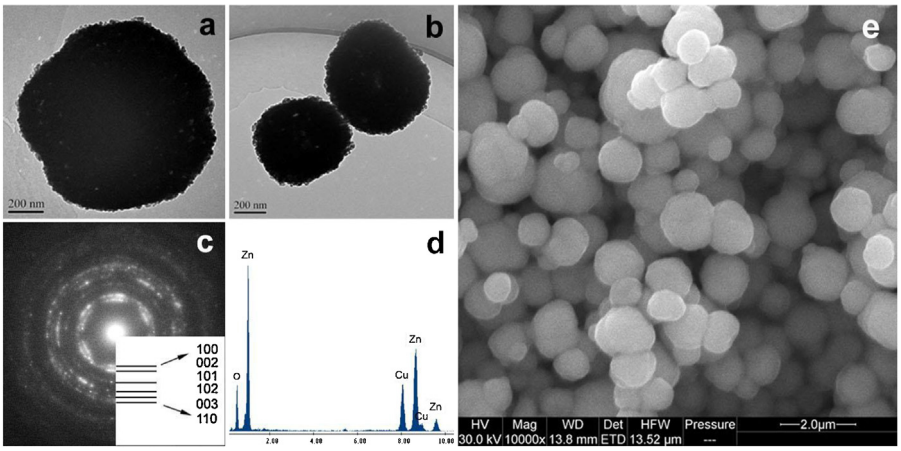

Fig. 4. Typical TEM images of ZnO microspheres (a,b); the SAED pattern of the ZnO microspheres showing diffraction circles corresponding to (1 0 0), (0 0 2), (1 0 1), (1 0 2), (0 0 3) and (1 1 0) planes of the wurtzite ZnO (c); and typical EDS spectra from the same single microsphere (d). SEM image of the ZnO microspheres (e).

be electrostatic interaction between CMGP with negative charges and QGP with positive charges. To verify the stepwise deposition of two polyelectrolytes, the changes in the surface zeta potential of the colloidal CMGP/QGP coated microspheres during the assembly process were characterized. Fig. 5a shows the variation of the zeta (ζ) potential of the coated microspheres as a function of the number of deposited polyelectrolyte layers. The ζ-potential value for the original ZnO particles was +30.1 mV. When adsorbed with one layer of anionic polyelectrolyte CMGP, the surface ζ-potential changed to −17.0 mV. Then with the adsorption of a layer of cationic polyelectrolyte QGP, the ζ-potential became +28.0 mV. With alternately adsorption of oppositely charged polyelectrolytes, the ζ-potential values varied periodically between positive and negative. The results demonstrated strongly that the CMGP/QGP realized layer-by-layer assembly on the surface of the ZnO microspheres. Since the charges of the polyelectrolyte monolayer deposited onto colloidal particles were the same, the electrostatic force between chains made the adsorption capacity increased hardly, and to some extent became saturated, thus ensuring the shell stability.

To provide additional direct evidences on the structure of the ZnO/CMGP/QGP core–shell microspheres, TEM was used to investigate the morphology of the microspheres. Fig. 6 shows the typical TEM images of the core–shell composite microspheres with different layers assembled by alternating deposition of CMGP and QGP onto ZnO microspheres. All the composite microspheres with different shell layers, such as ZnO/(CMGP/QGP) with two layers, ZnO/(CMGP/QGP)$_2$/CMGP with five layers and ZnO/(CMGP/QGP)$_3$/CMGP with seven layers exhibited typical core–shell structure. Clearly, the difference in the contrast between the ZnO core and the CMGP/QGP multilayers shell was the result of the orderly assembly of oppositely charged polyelectrolytes alternately deposited onto the ZnO microsphere surface by electrostatic attraction. It was noted that the self-assembly process was carried out in 0.5 M NaCl aqueous solution, so the inorganic salts would partially shield the ionic groups of the polyelectrolytes, leading to the reduction of the electrostatic repulsion. When adsorbed to the oppositely charged surface, the coiling chain conformation made it difficult to tile on the surface, eventually leading to the surface with non-uniform morphology and increasing roughness (Lvov, Ariga, Ichinose, & Kunitake, 1996; Schmitt et al., 1997). With an increasing number of deposited polyelectrolyte layers, the shell thickness exhibited a regular growth. The TEM results revealed that the shell thickness was about 48 nm for two layers; 101 nm for five layers; 145 nm for seven layers, respectively. Thus, the average polyelectrolyte monolayer thickness could be calculated to be ~20–24 nm. These results indicated that the alternating deposition of the polyelectrolyte had a growth rate of layer thickness, which was consistent with the number of layers.

Fig. 5b shows the hydrodynamic radius distribution of the microspheres before and after the CMGP/QGP multilayer deposition. In the absence of the adsorbed polyelectrolytes, its hydrodynamic radius (R_h) of the ZnO microspheres was 348 nm, or a diameter of about 700 nm. However, for the microspheres with eight adsorbed layers of polyelectrolytes, the size of the ZnO/(CMGP/QGP)$_4$ microspheres exhibited significant growth to give the R_h value of 565 nm. From the data of DLS, the average monolayer thickness could be calculated to be about 27 nm, very close to that obtained from TEM. The DLS results further supported

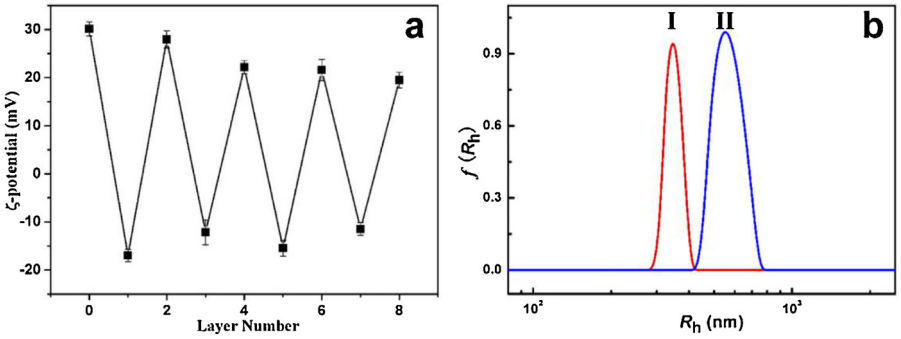

Fig. 5. (a) ζ-potential as a function of layer number for ZnO particles coated with alternatively CMGP (odd) and QGP (even) as the outer layer. The line is to guide the eye and has no physical meaning. (b) Hydrodynamic radius distribution [$f(R_h)$] of colloidal ZnO particles (I) and ZnO particles coated with eight-layer polyelectrolytes (II) in aqueous solution at 25 °C.

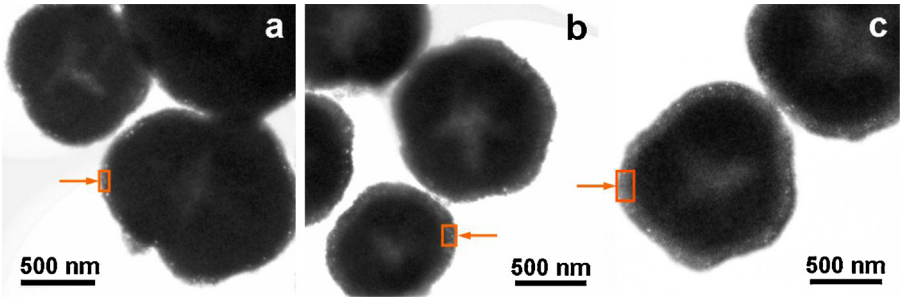

Fig. 6. TEM micrographs of colloidal ZnO particles coated with different layers of CMGP/QGP (a: 2 layers; b: 5 layers; c: 7 layers). Regular growth of the polyelectrolyte multilayers can be clearly seen, evidenced by an increase in the thickness of the polyelectrolyte shell.

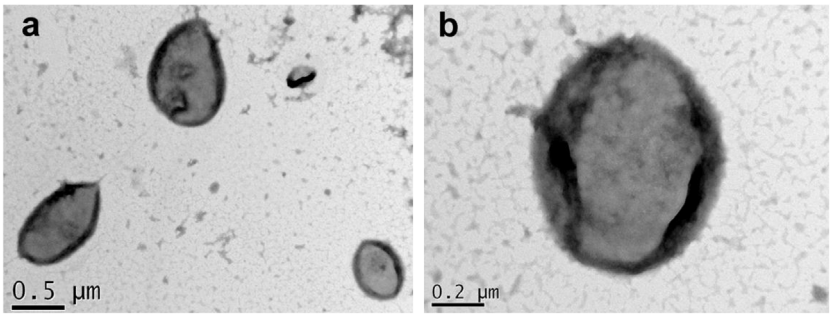

Fig. 7. TEM micrographs of CMGP/QGP hollow microcapsules with different magnification.

strongly that the polyelectrolyte monolayer adsorbed by the colloidal ZnO particle had a thickness of ~25 nm.

3.5. Creation of hollow microcapsules

Fig. 7 shows the TEM images of the microcapsules stained by 0.1% (w/v) phosphotungstic acid aqueous at different magnifications. The stained polyelectrolyte layer surrounding the less stained shell interior can be clearly identified. Interestingly, after the removal of the ZnO template, the hollow microcapsules collapsed into an ellipsoidal shape, and the capsule size was reduced slightly but still comparable with the core–shell composite microspheres. Moreover, the hollow capsules were found to be intact, indicating that the removal of the ZnO core did not rupture the microcapsule. The capsule deformation was a result of the large osmotic pressure between the inside and outside of the capsule during core removal process, which commonly exists in the preparation of polyelectrolyte capsules. The folds in the surface of the capsules were generated by drying during the preparation. The proteins, nucleic acids, drugs and other active substances could be easily encapsulated in the hydrophilic microcapsules, providing the potential applications in the field of controlled drug-delivery.

On the basis of the results described in previous sections, a schematic description of the assembly of the quaternized polysaccharide and the carboxymethyl polysaccharide by alternate deposition onto the ZnO particles is proposed in Fig. 8. As shown in Fig. 8 (a), the colloidal ZnO particles with positive charge was added firstly into the excess negatively charged CMGP solution, leading to the adsorption of CMGP on the surface of the ZnO particles, supported by the results in Fig. 5a. After the excess CMGP was removed by centrifugation and washing, a positively charged QGP solution was selected to repeat the process. As shown in Fig. 8b and c, the oppositely charged polyelectrolytes were stepwisely adsorbed on the surface of the ZnO particles, forming the composite microspheres with ZnO as the core and CMGP/QGP as the shells, supported by the results in Figs. 5 and 6. Finally, the microcapsules were constructed by removing the ZnO core, as shown

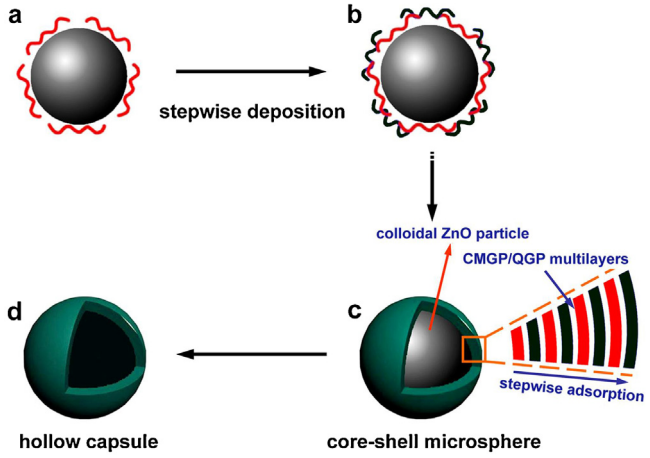

Fig. 8. Schematic illustration of the polysaccharide-based polyelectrolytes deposition progress and of the subsequent core decomposition. The red and dark green molecules represent polyanions and polycations, respectively. (For interpretation of the references to color in this figure legend, the reader is referred to the web version of this article.)

in Fig. 8d. The hollow microcapsules were confirmed by the data from DLS and TEM in Figs. 5b and 7. It is well reported that the *G. lucidum* polysaccharide is a β-glucan with excellent bioactivity and biocompatibility as well as non-toxic side effects. Therefore, the hollow microcapsules constructed by the glucan derivatives have a great potential in the drug-delivery systems.

4. Conclusion

A water-insoluble linear β-(1 → 3)-D-glucan was successfully used as raw material to synthesize the carboxymethyl polysaccharides (CMGP) and the quaternary ammonium polysaccharides (QGP) in the NaOH aqueous solution. The CMGP and QGP samples

were water-soluble, and showed a typical polyelectrolyte effect in aqueous solution as a result of strong electrostatic force. Thus, the negatively charged CMGP and the positively charged QGP were alternately layer-by-layer deposited easily on the surface of the ZnO colloidal particles with positive charge, leading to the formation of the multilayered composite microspheres. The thickness of the shell could be controlled by the number of layers of the CMGP and QGP polyelectrolytes alternately deposited, and increased from 48 to 145 nm with an increase of the number of layers from two to seven. The CMGP/QGP hollow microcapsules were constructed by removing the ZnO core with acetic acid. Due to the beneficial health properties of the β-D-glucans, the CMGP/QGP hollow microcapsules were safe and biocompatible, that will have potential applications in the field of controlled drug release.

Acknowledgments

This work was supported by the National Basic Research Program of China (973 Program, 2010CB732203), and the National Natural Science Foundation of China (20874079, 20904043). We acknowledged the Center of Nanoscience and Nanotechnology, and the Center for Electron Microscope of Wuhan University for their technical support.

References

Ackern, F., Krasemann, L., & Tieke, B. (1998). Ultrathin membranes for gas separation and pervaporation prepared upon electrostatic self-assembly of polyelectrolytes. *Thin Solid Films*, *327/329*, 762–766.

Ariga, K., Lvov, Y., & Kunitake, T. (1997). Assembling alternate dye-polyion molecular films by electrostatic layer-by-layer adsorption. *Journal of the American Chemical Society*, *119*, 2224–2231.

Cao, L., & Lin, Z. (2002). Regulation on maturation and function of dendritic cells by *Ganoderma lucidum* polysaccharides. *Immunology Letters*, *83*, 163–169.

Caruso, F., Caruso, R. A., & Möhwald, H. (1998). Nanoengineering of inorganic and hybrid hollow spheres by colloidal templating. *Science*, *282*, 1111–1114.

Caruso, F., Furlong, D. N., Ariga, K., Ichinose, I., & Kunitake, T. (1998). Characterization of polyelectrolyte–protein multilayer films by atomic force microscopy, scanning electron microscopy, and Fourier transform infrared reflection–absorption spectroscopy. *Langmuir*, *14*, 4559–4565.

Caruso, F., Lichtenfeld, H., Giersig, M., & Möhwald, H. (1998). Electrostatic self-assembly of silica nanoparticle–polyelectrolyte multilayers on polystyrene latex particles. *Journal of the American Chemical Society*, *120*, 8523–8524.

Chang, C., He, M., Zhou, J., & Zhang, L. (2011). Swelling behaviors of pH- and salt-responsive cellulose-based hydrogels. *Macromolecules*, *44*, 1642–1648.

Chluba, J., Voegel, J., Decher, G., Erbacher, P., Schaaf, P., & Ogier, J. (2001). Peptide hormone covalently bound to polyelectrolytes and embedded into multilayer architectures conserving full biological activity. *Biomacromolecules*, *2*, 800–805.

Chung, A. J., & Rubner, M. F. (2002). Methods of loading and releasing low molecular weight cationic molecules in weak polyelectrolyte multilayer films. *Langmuir*, *18*, 1176–1183.

Colson, P., Jennings, H. J., & Smith, I. C. P. (1974). Composition, sequence, and conformation of polymers and oligomers of glucose as revealed by carbon-13 nuclear magnetic resonance. *Journal of the American Chemical Society*, *96*, 8081–8087.

Czop, J. K., & Austen, K. F. (1985a). A beta-glucan inhibitable receptor on human monocytes: Its identity with the phagocytic receptor for particulate activators of the alternative complement pathway. *The Journal of Immunology*, *134*, 2588–2593.

Czop, J. K., & Austen, K. F. (1985b). Properties of glycans that activate the human alternative complement pathway and interact with the human monocyte beta-glucan receptor. *The Journal of Immunology*, *135*, 3388–3393.

Czop, J. K., & Kay, J. (1991). Isolation and characterization of beta-glucan receptors on human mononuclear phagocytes. *The Journal of Experimental Medicine*, *173*, 1511–1520.

Decher, G. (1997). Fuzzy nanoassemblies: Toward layered polymeric multicomposites. *Science*, *277*, 1232–1237.

Decher, G., Hong, J. D., & Schmitt, J. (1992). Buildup of ultrathin multilayer films by a self-assembly process: III. Consecutively alternating adsorption of anionic and cationic polyelectrolytes on charged surfaces. *Thin Solid Films*, *210/211*, 831–835.

Donath, E., Sukhorukov, G. B., Caruso, F., Davis, S. A., & Möhwald, H. (1998). Novel hollow polymer shells by colloid-templated assembly of polyelectrolytes. *Angewandte Chemie International Edition*, *37*, 2201–2205.

Elisseeff, J. (2008). Hydrogels: Structure starts to gel. *Nature Materials*, *7*, 271–273.

Ferreira, M., Cheung, J. H., & Rubner, M. F. (1994). Molecular self-assembly of conjugated polyions: A new process for fabricating multilayer thinfilm heterostructures. *Thin Solid Films*, *244*, 806–809.

Fuoss, R. M., & Strauss, U. P. (1948). Polyelectrolytes, II. Poly-4-vinylpyridonium chloride and poly-4-vinyl-*N*-*n*-butylpyridonium bromide. *Journal of Polymer Science*, *3*, 246–263.

He, J., Valluzzi, R., Yang, K., Dolukhanyan, T., Sung, C., Kumar, J., et al. (1999). Electrostatic multilayer deposition of a gold–dendrimer nanocomposite. *Chemistry of Materials*, *11*, 3268–3274.

Hiller, S., Leporatti, S., Schnäckel, A., Typlt, E., & Donath, E. (2004). Protamine assembled in multilayers on colloidal particles can be exchanged and released. *Biomacromolecules*, *5*, 1580–1587.

Huggins, M. L. (1942). The viscosity of dilute solutions of long-chain molecules. IV. Dependence on concentration. *Journal of the American Chemical Society*, *64*, 2716–2718.

Jiang, S., & Liu, M. (2004). A chiral switch based on dye-intercalated layer-by-layer assembled DNA film. *Chemistry of Materials*, *16*, 3985–3987.

Kacurakova, M., Ebringerova, A., Hirsch, J., & Hromadkova, Z. (1994). Infrared study of arabinoxylans. *Journal of the Science of Food and Agriculture*, *66*, 423–427.

Kiho, T., Sakushima, M., Wang, S., Nagai, K., & Ukai, S. (1991). Polysaccharides in fungi, XXVI. Two branched (1 → 3)-β-D-glucans from hot water extract of Yu er. *Chemical Pharmaceutical Bulletin*, *39*, 798–800.

Kong, W., Zhung, X., Gao, M., Zhou, H., Li, W., & Shen, J. (1994). A new kind of immobilized enzyme multilayer based on cationic and anionic interaction. *Macromolecular Rapid Communications*, *15*, 405–409.

Ladet, S., David, L., & Domard, A. (2008). Multi-membrane hydrogels. *Nature*, *452*, 76–79.

Lapasin, R., & Pricl, S. (1995). Rheology of polysaccharide systems. In *Rheology of industrial polysaccharides: Theory and applications*. Glasgow: Blackie.

Laschewsky, A., Mayer, B., Wischerhoff, E., Arys, X., Bertrand, P., Delcorte, A., et al. (1996). A new route to thin polymeric, non-centrosymmetric coatings. *Thin Solid Films*, *284/285*, 334–337.

Li, C.-S., Li, Y.-N., Wu, Y.-L., Ong, B.-S., & Loutfy, R.-O. (2009). Fabrication conditions for solution-processed high-mobility ZnO thin-film transistors. *Journal of Materials Chemistry*, *19*, 1626–1634.

Loubaki, E., Ourevitch, M., & Sicsic, S. (1991). Chemical modification of chitosan by glycidyl trimethylammonium chloride. Characterization of modified chitosan by ^{13}C- and ^{1}H-NMR spectroscopy. *European Polymer Journal*, *27*, 311–317.

Lvov, Y., Ariga, K., Ichinose, I., & Kunitake, T. (1996). Molecular film assembly via layer-by-layer adsorption of oppositely charged macromolecules (linear polymer, protein and clay) and concanavalin A and glycogen. *Thin Solid Films*, *284–285*, 797–801.

Lvov, Y., Kamau, G., Zhou, D., & Rusling, J. (1999). Assembly of electroactive ordered multilayer films of cobalt phthalocyanine tetrasulfonate and polycations. *Journal of Colloid and Interface Science*, *212*, 570–575.

Lvov, Y., Lu, Z., Schenkman, J. B., Zu, X., & Rusling, J. F. (1998). Direct electrochemistry of myoglobin and cytochrome P450 cam in alternate layer-by-layer films with dna and other polyions. *Journal of the American Chemical Society*, *120*, 4073–4080.

Lvov, Y., & Sukhorukov, G. B. (1997). Protein architecture: Assembly of ordered films by means of alternated adsorption of oppositely charged macromolecules. *Membrane & Cell Biology*, *11*, 277–303.

Mitchell, J. R. (1979). Rheology of polysaccharides solutions and gels. In J. M. V. Blanshard, & J. R. Mitchell (Eds.), *Polysaccharide in foods* (pp. 51–72). London: Butterworths.

Ostrander, J. W., Mamedov, A. A., & Kotov, N. A. (2001). Two modes of linear layer-by-layer growth of nanoparticle-polyelectrolyte multilayers and different interactions in the layer-by-layer deposition. *Journal of the American Chemical Society*, *123*, 1101–1110.

Pal, S., Mal, D., & Singh, R. P. (2005). Cationic starch: An effective flocculating agent. *Carbohydrate Polymers*, *59*, 417–423.

Pei, R., Cui, X., Yang, X., & Wang, E. (2001). Assembly of alternating polycation and DNA multilayer films by electrostatic layer-by-layer adsorption. *Biomacromolecules*, *2*, 463–468.

Qiu, X., Leporatti, S., Donath, E., & Möhwald, H. (2001). Studies on the drug release properties of polysaccharide multilayers encapsulated ibuprofen microparticles. *Langmuir*, *17*, 5375–5380.

Rogach, A. L., Koktysh, D. S., Harrison, M., & Kotov, N. A. (2000). Layer-by-layer assembled films of HgTe nanocrystals with strong infrared emission. *Chemistry of Materials*, *12*, 1526–1528.

Schmitt, J., Decher, G., Dressick, W. J., Brandow, S. L., Geer, R. E., Sashidhar, R., et al. (1997). Metal nanoparticle/polymer superlattice films: Fabrication and control of layer structure. *Advanced Materials*, *9*, 61–65.

Serizawa, T., Yamaguchi, M., & Akashi, M. (2003). Time-controlled desorption of ultrathin polymer films triggered by enzymatic degradation. *Angewandte Chemie International Edition*, *42*, 1115–1118.

Sukhorukov, G. B., Donath, E., Davis, S., Lichtenfeld, H., Caruso, F., Popov, V. I., et al. (1998). Stepwise polyelectrolyte assembly on particle surfaces: A novel approach to colloid design. *Polymers for Advanced Technologies*, *9*, 759–767.

Sukhorukov, G. B., Donath, E., Lichtenfeld, H., Knippel, E., Knippel, M., Budde, A., et al. (1998). Layer-by-layer self assembly of polyelectrolytes on colloidal particles. *Colloids and Surfaces A: Physicochemical and Engineering Aspects*, *137*, 253–266.

Sun, G., & Chu, C.-C. (2009). Self-assembly of chemically engineered hydrophilic dextran into microscopic tubules. *ACS Nano*, *3*, 1176–1182.

Sun, Y., Hao, E., Zhang, X., Yang, B., Shen, J., Chi, L., et al. (1997). Buildup of composite films containing TiO_2/PbS nanoparticles and polyelectrolytes based on electrostatic interaction. *Langmuir*, *13*, 5168–5174.

Taton, T. A., Mucic, R. C., Mirkin, C. A., & Letsinger, R. L. (2000). The DNA-mediated formation of supramolecular mono- and multilayered nanoparticle structures. *Journal of the American Chemical Society*, *122*, 6305–6306.

Thierry, B., Winnik, F. M., Merhi, Y., Silver, J., & Tabrizian, M. (2003). Bioactive coatings of endovascular stents based on polyelectrolyte multilayers. *Biomacromolecules*, *4*, l564–l1571.

Van Cott, K. E., Guzy, M., Neyman, P., Brands, C., Heflin, J. R., Gibson, H. W., et al. (2002). Layer-by-layer deposition and ordering of low-molecular-weight dye molecules for second-order nonlinear optics. *Angewandte Chemie International Edition*, *41*, 3236–3238.

Vázquez, E., Dewitt, D. M., Hammond, P. T., & Lynn, D. M. (2002). Construction of hydrolytically-degradable thin films via layer-by-layer deposition of degradable polyelectrolytes. *Journal of the American Chemical Society*, *124*, 13992–13993.

Wang, J., & Zhang, L. (2009). Structure and chain conformation of five water-soluble derivatives of a β-D-glucan isolated from *Ganoderma lucidum*. *Carbohydrate Research*, *344*, 105–112.

Wang, J., Zhang, L., Yu, Y., & Cheung, P. C. K. (2009). Enhancement of antitumor activities in sulfated and carboxymethylated polysaccharides of *Ganoderma lucidum*. *Journal of Agricultural and Food Chemistry*, *57*, 10565–10572.

Wang, R., Xing, Y., Xu, J., & Yu, D. (2003). Fabrication and microstructure analysis on zinc oxide nanotubes. *New Journal of Physics*, *5*, 115.1–115.7.

Wang, Y., Zhang, L., & Ruan, D. (2004). Preparation and structure of five derivatives of β-(1 → 3)-D-glucan isolated from *Poria cocos sclerotium*. *Chinese Journal of Polymer Science*, *22*, 137–145.

Wang, Z., Sasaki, T., Muramatsu, M., Ebina, Y., Tanaka, T., Wang, L., et al. (2003). Self-assembled multilayers of titania nanoparticles and nanosheets with polyelectrolytes. *Chemistry of Materials*, *15*, 807–812.

Zhang, G., Liu, L., Zhao, Y., Ning, F., Jiang, M., & Wu, C. (2000). Self-assembly of carboxylated poly(styrene-*b*-ethylene-*co*-butylene-*b*-styrene) triblock copolymer chains in water via a microphase inversion. *Macromolecules*, *33*, 6340–6343.

Zhang, L., Zhang, M., Chen, J., & Zeng, F. B. (2001). Solution properties of antitumor carboxymethylated derivatives of α-(1 → 3)-D-glucan from *Ganoderma lucidum*. *Chinese Journal of Polymer Science*, *19*, 283–289.

Zhang, X., Gao, M., Kong, X., Sun, Y., & Shen, J. (1994). Build-up a new type of ultrathin film of porphyrin and phthalocyanine based on cation anionic electrostatic attraction. *Journal of the Chemical Society, Chemical Communications*, *9*, 1055–1056.

Zhou, H., Song, G. Q., Zhang, Y. X., Chen, J. Y., Jiang, M., Esch, T. E. H., et al. (2001). Hydrophobically modified polyelectrolytes, 4 synthesis and solution properties of fluorocarbon-containing poly(acrylic acid). *Macromolecular Chemistry and Physics*, *202*, 3057–3064.

Zhou, Y., & Li, Y. (2004). Layer-by-layer self-assembly of multilayer films containing DNA and Eu^{3+}: Their characteristics and interactions with small molecules. *Langmuir*, *20*, 7208–7214.

Zhu, A., Zhang, M., Wu, J., & Shen, J. (2002). Covalent immobilization of chitosan/heparin complex with a photosensitive hetero-bifunctional crosslinking reagent on PLA surface. *Biomaterials*, *23*, 4657–4665.